PNAS Nexus, 2024, 3, pgae312
https://doi.org/10.1093/pnasnexus/pgae312
Advance access publication 26 July 2024
Research Report

A structure-redesigned intrinsically disordered peptide that selectively inhibits a plant transcription factor in jasmonate signaling

Yousuke Takaoka [a,*], Ruiqi Liu [a] and Minoru Ueda [a,b]

[a]Department of Chemistry, Graduate School of Science, Tohoku University, 6-3, Aramaki-Aza Aoba, Aoba-ku, Sendai 980-8578, Japan
[b]Department of Molecular and Chemical Life Sciences, Graduate School of Life Sciences, Tohoku University, Sendai, Japan
*To whom correspondence should be addressed: Email: ytakaoka@tohoku.ac.jp
Edited By Josh Wand

Abstract

Plant hormone-related transcription factors (TFs) are key regulators of plant development, responses to environmental stress such as climate changes, pathogens, and pests. These TFs often function as families that exhibit genetic redundancy in higher plants, and are affected by complex crosstalk mechanisms between different plant hormones. These properties make it difficult to analyze and control them in many cases. In this study, we introduced a chemical inhibitor to manipulate plant hormone-related TFs, focusing on the jasmonate (JA) and ethylene (ET) signaling pathways, with the key TFs MYC2/3/4 and EIN3/EIL1. This study revealed that $JAZ10^{CMID}$, the binding domain of the repressor involved in the desensitization of both TFs, is an intrinsically disordered region in the absence of binding partners. Chemical inhibitors have been designed based on this interaction to selectively inhibit MYC TFs while leaving EIN3/EIL1 unaffected. This peptide inhibitor effectively disrupts MYC-mediated responses while activating EIN3-mediated responses and successfully uncouples the crosstalk between JA and ET signaling in *Arabidopsis thaliana*. Furthermore, the designed peptide inhibitor was also shown to selectively inhibit the activity of MpMYC, an ortholog of AtMYC in *Marchantia polymorpha*, demonstrating its applicability across different plant species. This underscores the potential of using peptide inhibitors for specific TFs to elucidate hormone crosstalk mechanisms in non-model plants without genetic manipulation. Such a design concept for chemical fixation of the disordered structure is expected to limit the original multiple binding partners and provide useful chemical tools in chemical biology research.

Keywords: transcription factors, intrinsically disordered region, chemical biology, jasmonate pathway

Significance Statement

Transcription factors (TFs) are essential for plants to respond to environmental changes; however, their redundancy and complex interactions make studying them challenging. We aimed to design chemical inhibitors to selectively target and manipulate TFs involved in jasmonate and ethylene signaling, particularly MYC2/3/4 and EIN3/EIL1. Based on the molecular interactions between these TFs and the intrinsically disordered region of repressor JAZ proteins, we successfully developed a structure-redesigned stapled peptide that selectively inhibited MYC activity without affecting EIN3. This peptide inhibitor showed promise in *Arabidopsis thaliana* and *Marchantia polymorpha*, demonstrating its potential as a versatile tool for studying plant hormone signaling and crosstalk across different plant species.

Introduction

Plant hormone-related transcription factors (TFs) are key regulators of the plant life cycle, including germination, growth, differentiation, and senescence (1). Because these TFs play pivotal roles in sessile plants' adaptation to environmental changes, they are often genetically redundant during the evolution process to be robust against unexpected mutations (1, 2). When such TF family members are involved in the function redundantly, it is necessary to comprehensively analyze or control almost all homologs to investigate the functions of them. In this situation, using conventional genetic or transcriptional approaches is time-consuming and must be done for each plant species. Furthermore, a crosstalk regulatory system occurs between specific TFs, making analysis difficult (3, 4). Based on this background, chemical tools that control plant hormone-related TFs are expected to be effective alternatives for analyzing plant hormone

Competing Interest: The authors declare no competing interests.
Received: April 29, 2024. **Accepted:** July 10, 2024

signaling. Therefore, in this study, we aimed to develop such useful inhibitor that acts selectively on all members of the target TF family in a wide range of plant species.

Jasmonate (JA) is a plant hormone that contributes to the regulation of plant defense responses (5). JA signaling is mediated by MYC TFs, which are master regulator TFs for anti-insect defense responses (6, 7). It has been demonstrated that many JA responses such as plant stamen development, seed production, senescence, and glucosinolate biosynthesis are redundantly regulated by MYC2/3/4 or MYC2/3/4/5 (8–11), although recent reports have also revealed that MYC2 specifically regulates partial JA responses such as tryptophan metabolism nonredundantly (12, 13). Jasmonoyl-L-isoleucine (JA-Ile), a bioactive form of JA in higher plants, causes a protein–protein interaction (PPI) between the F-box protein CORONATINE INSENSITIVE 1 (COI1) and the Jas motif, a C-terminal degron sequence of the JASMONATE-ZIM DOMAIN (JAZ) repressor protein that triggers ubiquitination and subsequent degradation of JAZ through the 26S proteasome pathway (14, 15). In the absence of JA-Ile, the JAZ Jas motif binds to and represses various JA-related TFs, including MYC (16). In contrast, when JA-Ile is biosynthesized in plants under biotic or abiotic stress, MYC is derepressed and subsequently activated by binding to the transcriptional mediator MED25 to upregulate the expression of various marker genes involved in defense responses, secondary metabolite production, fertility, senescence, and growth inhibition (17–19). Activated MYC is desensitized by accumulating several JAZ splice variants, such as JAZ10.3 (lacking the C-terminus of the Jas motif) and JAZ10.4 (lacking the entire Jas motif). These splice variants contain an N-terminal cryptic MYC interaction domain (CMID) that strongly interacts with MYC to desensitize MYC-associated target gene expression (20–23). Quantitative binding assays revealed that the order of binding affinity between MYC3 and its binding partners, $JAZ^{Jas} < MED25^{CMIDM} < JAZ^{CMID}$, was beneficial for efficient signal transduction (24).

ETHYLENE INSENSITIVE 3 (EIN3) is a master regulator of defense responses against pathogen infections in JA and ethylene (ET) signaling (25, 26). Notably, most of the regulators of EIN3 are shared with JA signaling, that is, EIN3 is also suppressed by the Jas motif of the JAZ protein and activated through binding with MED25 (25, 27, 28). In addition, MYC2 and EIN3 mutually antagonize their respective downstream responses (29, 30). Unsurprisingly, MYC and EIN3 have multiple functionally redundant homologs in *Arabidopsis thaliana* (MYC2/3/4/5 and EIN3/EIN3-LIKE PROTEIN1 [EIL1], respectively) (10, 25).

While MYC desensitization has been thoroughly investigated (20–23), the desensitization of EIN3 has not been previously analyzed. Therefore, we analyzed the desensitization stages of MYC and EIN3 at the molecular level and confirmed that both TFs were desensitized through interactions with $JAZ10^{CMID}$. Moreover, we found that $JAZ10^{CMID}$ alone is an intrinsically disordered region (IDR) in the buffer solution, and this region was found to interact with different binding partners MYC and EIN3 families. Based on these findings, we designed chemically stapled helical peptides that mimic the binding form of $JAZ10^{CMID}$ complexed with MYC3. This CMID-based stapled peptide selectively inhibited MYC3 but not EIN3. In addition, the designed peptide inhibitor comprehensively inhibited MYC2/3/4, but not EIN3/EIL1, resulting in the uncoupling of the crosstalk between JA and ET in *A. thaliana*. Furthermore, our designed peptide also functions as a useful inhibitor of a MYC ortholog in the primitive liverworts *Marchantia polymorpha*, demonstrating the general applicability of this peptide inhibitor for plant hormone-related TFs.

Materials and methods

General materials and methods

All chemical reagents and solvents were obtained from commercial suppliers (Wako Pure Chemical Industries Co. Ltd, Nacalai Tesque Co., Ltd, Watanabe Chemical Industries Co. Ltd, Thermo Fisher Scientific K.K., GE Healthcare, Sigma-Aldrich Co. LLC, KISHIDA CHEMICAL Co., Ltd, Kanto Chemical Co. Ltd, Nippon Gene Co. Ltd) and used without further purification. UV–Vis spectra were recorded on a UV-2600 spectrophotometer (Shimadzu, Kyoto, Japan). Circular dichroism spectra were recorded on a J-820 (JASCO, Tokyo, Japan). Fluorescence spectra and anisotropy were recorded on a FP-8500 (JASCO). Reverse-phase HPLC was carried out on a PU-4180 plus equipped with UV-4075 and MD-4010 detectors (JASCO). Absorbance at 220 and 540 nm was monitored by an MD-4010 photodiode array detector. MALDI-TOF MS analysis was performed on an Autoflex Speed (Bruker Daltonics Inc., MA, USA). The 3D structures were constructed using MOE 2020.0901 software (Chemical Computing Groups, Montreal, Canada). The AlphaLISA assay was carried out on an EnVision (PerkinElmer, Inc., USA). SDS–PAGE and western blotting were analyzed with a Mini-Protean III electrophoresis apparatus (Bio-Rad, Hercules, CA, USA). Chemiluminescent signals were detected with an Amersham Imager 680 detector (GE Healthcare, CA, USA). Seedling photographs were taken with a digital single-lens reflex camera α6400 (Sony Corp., Tokyo, Japan). Quantitative RT-PCR analysis was carried out on a QuantStudio Real-Time PCR System (Thermo Fisher Scientific, USA). Quantification of secondary metabolites (glucosinolate and coumaroyl agmatine) was carried out on the Ultivo Triple Quadrupole LC/MS system (Agilent Technologies, Inc., Santa Clara, USA). The transformation of 35S:JAZ10.4-EYFP seedlings was confirmed by confocal laser scanning microscopy analyses (LSM700, Carl Zeiss Co., Ltd, GE) using laser line 488 nm.

FA measurement

FA titration experiments were performed at 25°C in 20 mM Tris–HCl buffer (pH 8.0, 200 mM NaCl, 10% glycerol, 10% cOmplete EDTA-Free in the absence [for MYC family] or presence [for EIN3/EIL1 family] of 2-mercaptoethanol) using a quartz cell (150 μL) as previously described (Table S1). FA intensities were measured ($\lambda_{ex}/\lambda_{em}$ = 543 nm/573.5 nm for tetramethylrhodamine). Protein solution was added dropwise to the solution containing TMR-conjugated JAZ peptide (100 nM). FA values (r) were calculated using the following equation: $r = (I_{VV} - G \times I_{VH})/(I_{VV} + 2G \times I_{VH})$ where I_{VV} and I_{VH} are the fluorescence intensities observed through polarizers parallel and perpendicular to the polarization of the exciting light, respectively, and G is a correction factor to account for instrumental differences in detecting emitted compounds ($G = I_{HV}/I_{HH}$). An average value of three independent measurements was calculated for each point. Anisotropy titration curves were analyzed with the nonlinear curve-fitting analysis to evaluate apparent K_a and K_d values.

Plant materials and growth conditions

A. thaliana Col-0 is the genetic background of wild-type and mutant lines used in this study. *A. thaliana* seeds were surface-sterilized and vernalized for 2–3 days at 4°C. All Arabidopsis seedlings were grown under 16-h light (75 μmol m^{-2} s^{-1}; cool-white fluorescent light)/8-h dark cycle at 22°C on a half-strength Murashige–Skoog (MS) plate (2% sucrose, 0.4% gellan gum) or liquid medium (0.5% sucrose) in a cultivation chamber CL-301 (TOMY SEIKO Co., Ltd, Tokyo, Japan).

Agrobacterium GV3101, containing *pEarleygate101-JAZ10.4-EYFP* (kindly gifted from Prof. Gregg Howe and Dr Jian Yao, Michigan State University, USA), was used to transform Col-0 plants by conventional floral dipping methods. The transformed plants were grown on half-strength MS plates, and after 6 and 8 days, they were sprayed twice with 250 μM BASTA and 0.05% Silwet L-77 dissolved in half-strength MS liquid medium to select transgenic lines (T1 generation). These T1 plants (10 days old) were transferred to fresh half-strength MS liquid medium for subsequent RT-qPCR experiments (12-day-old seedlings were used in this study). The transformation was confirmed by confocal microscopic observation of roots and RT-qPCR with specific primers (*JAZ10.4-EYFP* shown in Table S2).

M. polymorpha accession Takaragaike-1 (Tak-1) was used as wild type. *M. polymorpha* plants were grown on half-strength Gamborg's B5 medium containing 1% agar under continuous light (50–60 μmol m^{-2} s^{-1}; cool-white fluorescent light) at 22°C.

Quantitative RT-PCR analyses for *A. thaliana* and *M. polymorpha*

For Arabidopsis seedlings, MeJA and/or peptides were treated to 7-day-old plants in half-strength MS liquid medium. Each chemical was treated for 2 h (for *AOS*, *OPR3*, *MYC2*, and *ORA59*) or 8 h (for *VSP2*, *PDF1.2*, and *ACT*). Total RNA was isolated using an ISOGEN kit (Nippon Gene, Japan), and then, first-strand cDNA was gained with ReverTra Ace reverse transcriptase (Toyobo, Japan) with oligo-dT primers. For *Marchantia* seedlings, OPDA (Cayman Chemical, MI, USA) and/or peptides were treated to 7-day-old gemmalings on a cloth suspended in half-strength Gamborg's B5 liquid medium and 6-h incubation. Total RNA was isolated using NucleoSpin RNA kit (MACHEREY-NAGEL GmbH & Co KG, Germany), and then, first-strand cDNA was gained as above shown. A QuantStudio III Real-Time PCR System (Life Technologies, USA) was used for quantitative PCR (all primers sequences for qPCR are shown in Tables S2 and S3). Polyubiquitin 10 was used as a reference gene for Arabidopsis seedlings. *MpEF1α* was used as a reference gene for *Marchantia* seedlings.

Results

JAZ10.4 splice variant is involved in the desensitization of MYC- and EIN3-downstream responses

We previously demonstrated that the binding affinity of the PPI involved in MYC-associated JA signaling becomes stronger the further downstream, that is, the PPI between MYC and JAZ^{Jas} at the resting stage, followed by the PPI between MYC and $MED25^{CMIDM}$ at the activation stage, and the last PPI between MYC and JAZ^{CMID} at the desensitization stage (24). Quantitative analyses by fluorescence anisotropy (FA) revealed that the dissociation constants between MYC3 and its counterpart peptides conjugated with the fluorophores (fluorescein [Fl] or tetramethyl rhodamine [TMR]), TMR-$JAZ9^{Jas}$, Fl-$MED25^{CMIDM}$, and TMR-JAZ^{CMID} were 5,000, 1,900, and 350 nM, respectively (Table S4 and Fig. S1a). In addition, $JAZ10^{CMID}$ can be replaced with $MED25^{CMIDM}$ at least in vitro, suggesting that $JAZ10^{CMID}$ functions effectively in the rapid desensitization of MYC during the late stage of the JA signaling. EIN3 is suppressed by JAZ^{Jas} and activated by $MED25^{CMIDM}$; however, no studies exist on whether it is desensitized by $JAZ10^{CMID}$, and therefore, the binding affinity between the $JAZ10^{CMID}$ and EIN3 was examined quantitatively. As shown in Fig. S1b, the K_d value between the $JAZ10^{CMID}$ peptide and EIN3 was 620 nM using FA experiments. This value was comparable to the affinity between $MED25^{CMIDM}$ and EIN3 (Table S4) (28). Considering these in vitro results and the previously reported dynamic change of protein abundance that the JAZ10.3 or JAZ10.4 splice variants accumulate in the late stage of the JA signaling, both MYC3 and EIN3 may be desensitized by direct interaction with $JAZ10^{CMID}$.

Previous studies have suggested that overexpression of the JAZ10.4 splice variant (35S:JAZ10.4-YFP) in *Arabidopsis* resulted in male sterility or suppression of JA-triggered growth inhibition (20, 22). In addition, as previously reported, we also confirmed that the overexpressed JAZ10.4-YFP protein was mainly localized in the nucleus by confocal laser scanning microscopy analyses and was not degraded even after treatment with methyl jasmonate (MeJA, a precursor of JA) for 2 h (data not shown) (20). Moreover, real-time quantitative PCR (RT-qPCR) was used to analyze the detailed JA-associated responses of this plant to MeJA administration. As shown in Figs. 1a and S2a–c, the expression of typical downstream genes of MYC, such as *VSP2*, *AOS*, *OPR3*, and *MYC2*, was confirmed to be notably suppressed in 35S:JAZ10.4-YFP plants compared to wild-type plants (*Col-0*). Similarly, EIN3/EIL1-downstream genes, such as *PDF1.2*, *ACT*, and *ORA59*, were also downregulated in 35S:JAZ10.4-YFP compared to *Col-0* (Figs. 1b and S2d and e). Our in vitro and in vivo analyses would suggest that the JAZ10.4 splice variant is involved in the desensitization of MYC as well as in other JA-related TFs such as EIN3/EIL1.

The previously reported crystal structure of the $JAZ10^{CMID}$/MYC3 complex demonstrated that $JAZ10^{CMID}$ composed of two α-helices (α1 and α2) and two loops (N-loop and α1-2 loop) make more extensive interactions with MYC3 than with the Jas single helix (Fig. 1c) (23, 31). This structure suggests that $JAZ10^{CMID}$ has over 60% helical structure and "the structure of $JAZ10^{CMID}$ alone," as predicted by AlphaFold method, is almost identical to the reported crystal structure of $JAZ10^{CMID}$ complexed with MYC3 (32, 33). However, the primary sequence of $JAZ10^{CMID}$ is enriched with hydrophilic polar amino acids; therefore, it is unlikely to be a typical helical region. In addition, we verified whether this region is ordered or disordered by two recently reported independent prediction methods (fIDPnn and intrinsically disordered protein [IDP]-ELM predictors, respectively) (34, 35) and found that almost the entire sequence of $JAZ10^{CMID}$ (26–58 residues in JAZ10.1) was an IDR in addition to the Jas motif (166–192 residues in JAZ10.1) (Fig. S3). This discrepancy between the AlphaFold-based, IDR-prediction-based methods, and CD spectra of both Jas motif (36) and CMID peptides may be because, as Alderson et al. recently reported, AlphaFold2 often predicts the IDR structure as a conditional folding state (upon binding with its counterpart or under other specific conditions) (37). The secondary structure of $JAZ10^{CMID}$ was confirmed using the CD spectrum of the solution. As shown in Fig. 1d, the spectrum indicated that $JAZ10^{CMID}$ alone in the buffer solution had a helix content of 18.4% and a random coil structure of 73.4%, indicating that most regions of $JAZ10^{CMID}$ would be an IDR. In contrast, the homology between MYC3 and EIN3 was very low at 13% (Fig. S4), and their structures were expected to be significantly different. In several cases, IDPs/IDRs can interact with various binding partners in cells because they can adopt a flexible structure in a solution (38). Both the binding and structural analyses of $JAZ10^{CMID}$ with MYC3 or EIN3 suggested that $JAZ10^{CMID}$, as an IDR, changes its 3D shape or interaction site and can bind to both TFs MYC3 and EIN3 with similar affinity (Fig. 1e).

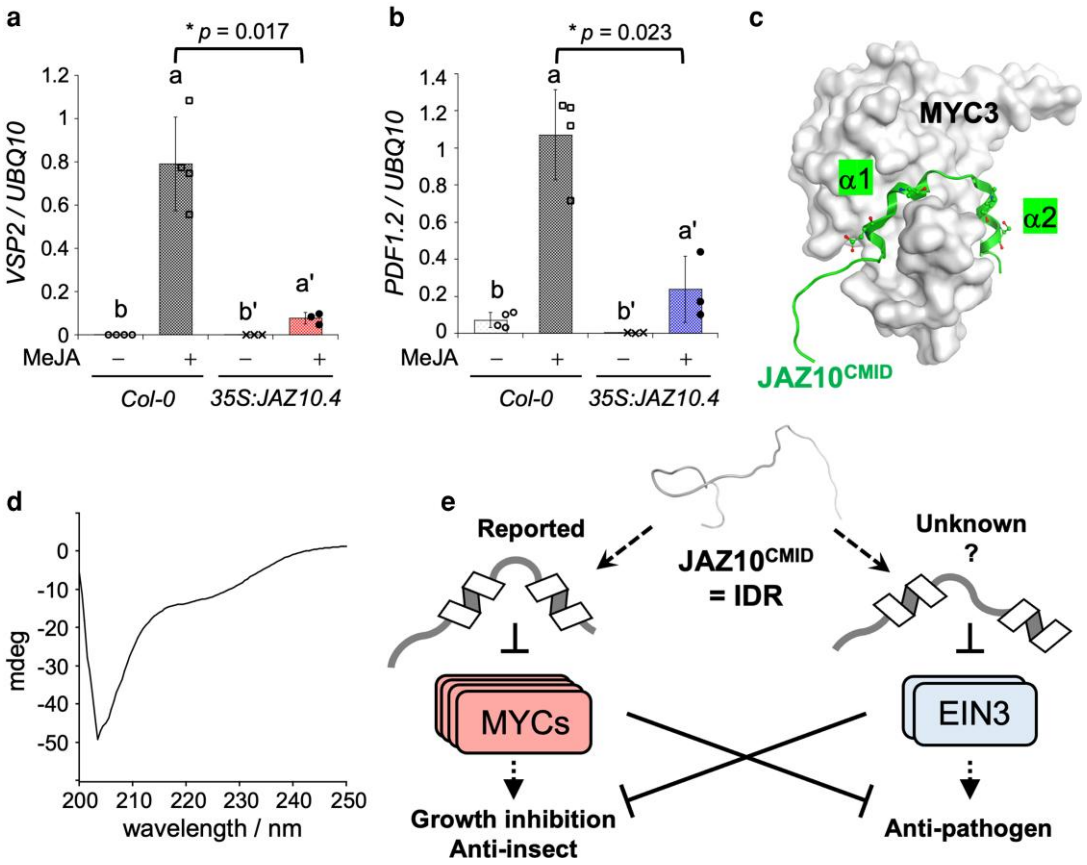

Fig. 1. JAZ10^{CMID} is an IDR that desensitizes MYC- and EIN3-downstream responses. a), b) Gene expression analyses of JA-responsive marker genes (a *VSP2*, b *PDF1.2*) using RT-qPCR in 12-day-old Arabidopsis seedlings (*Col-0* or *35S:JAZ10.4*) with or without MeJA (50 μM) ($n = 3$ or 4). Experiments were repeated three times with similar results, and significant differences were evaluated by one-way ANOVA/Tukey's HSD post hoc test ($P < 0.05$). c) The reported crystal structure of JAZ10^{CMID} (green ribbon) complexed with MYC3 (PDB ID: 5T0F). d) CD spectrum of TMR-CMID-wt (**1**, shown in Fig. 2a) in PBS buffer (pH 7.4). e) A predictive diagram shows how an IDR, JAZ10^{CMID}, suppresses MYCs and EIN3/EIL1 TFs by changing its 3D shape.

Structure-based chemical stapling of JAZ10^{CMID} provides a selective inhibitor for the MYC family

Based on the hypothesis shown in Fig. 1e, if the 3D structure of the JAZ10^{CMID} peptide is fixed in its binding form to MYC3, it can be predicted that the fixed peptide will bind selectively to MYC3 but not to EIN3. Moreover, IDRs often bind to their interaction partners while changing their structures, called the "coupled folding and binding" mechanism, and thus, fixing the 3D structure of JAZ10^{CMID} peptide to the binding form is expected to entropically favor binding with MYC3. Therefore, we designed classical stapled helical peptides by using an olefin metathesis reaction that mimicked the reported binding form of JAZ10^{CMID} with MYC3 (36, 39). From the crystal structure of the complex of JAZ10^{CMID} and MYC3, we found one pair of solvent-exposed i and $i+4$ amino acid in α1 (D38 and A42) that could be replaced with an *S*-form olefin-containing unnatural amino acid (Fig. 2a) (40, 41). In contrast, in the α2 helix, only the paired amino acids at positions i and $i+3$ (I50 and S53) were found to be exposed to the solvent, but not at positions i and $i+4$; therefore, they were replaced with *R*- and *S*-form olefin-containing ones, according to the previously reported strategy for helical stapling of i and $i+3$ amino acids (42) (Fig. 2a). Therefore, we designed and synthesized a non-stapled peptide (JAZ10^{CMID}-wt (**1**)), two single-stapled peptides for α1 and α2 (JAZ10^{CMID}-α1St (**2**), JAZ10^{CMID}-α2St (**3**)), and a double-stapled peptide (JAZ10^{CMID}-dSt (**4**)) (Fig. 2a). All peptides were synthesized using the Fmoc-based solid-phase synthesis method and covalently conjugated with the reporter TMR to examine their binding with TFs. They were purified by high-performance liquid chromatography (HPLC) and characterized by MALDI-TOF MS and ultraviolet–visible (UV–Vis) absorption spectra analyses (Fig. S5).

Before examining the inhibitory effects of the designed peptides, we performed in silico molecular docking simulations of **4** and MYC3. As shown in Fig. 2b, double-stapled peptide **4** bound to MYC3 without perturbation of this interaction at the stapling sites of **4**. Next, to examine the binding affinity of these stapled peptides for MYC3 and EIN3, we newly prepared the JAZ-binding domains of them tethering both His6-SUMO-tag and FLAG-tag for purification and detection with FA and AlphaScreen as conventionally used PPI assays (His6-SUMO-MYC3(44–238)-FLAG (His-MYC3-FLAG) or His6-SUMO-EIN3(200–500)-FLAG (His-EIN3-FLAG), Fig. S6). According to our previous studies, the binding affinities of these peptides to TFs were quantitatively examined using FA assays (24, 36). The apparent K_d value of **1** with His-MYC3-FLAG was calculated to be 210 nM, which is similar to that of a previously reported complex of Fl-conjugated JAZ10^{CMID}-wt and His-MYC3 (350 nM). In contrast, the K_d values of **2**, **3**, and **4** with His-MYC3-FLAG were 61, 310, and 5 nM, which are 7-, 0.67-, and 42-fold lower than that of **1**, respectively (Fig. 2c and Table S5). A similar enhancement in the affinity of double-stapled peptide **4** compared to non-stapled peptide **1** was also observed using the binding domains of MYC3 isoforms His-MYC2(55–287)-FLAG and His-MYC4(55–253)-FLAG (Figs. S7 and S8 and Table S5). This was reasonable because the primary

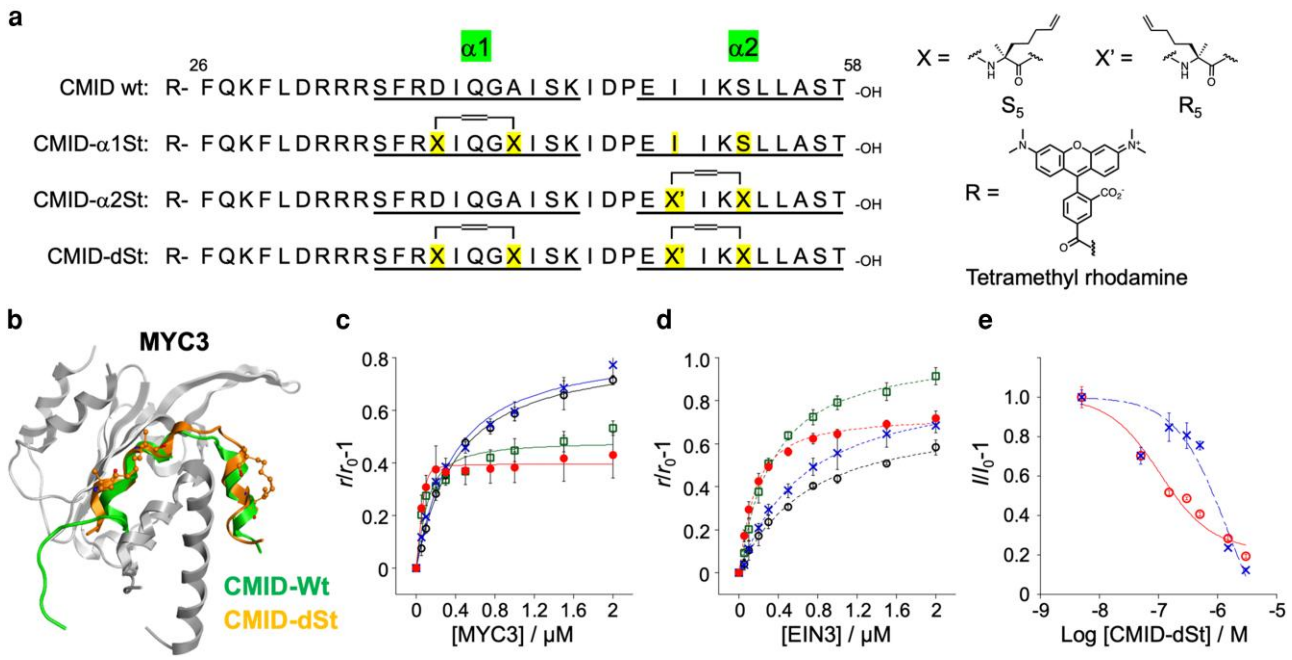

Fig. 2. Molecular design and binding analyses of the stapled peptides based on the JAZ10^{CMID} complex with MYC3. a) The amino acid sequences of stapled and non-stapled JAZ10^{CMID} peptides (non-stapled peptide CMID-wt (**1**), single-stapled peptides CMID-α1St (**2**) and CMID-α2St (**3**), and double-stapled peptide CMID-dSt (**4**), respectively), and chemical structures of the building block for stapling (*X* or *X'*) and TMR (R). b) The superimposed 3D structures of the reported crystal structure of MYC3 (gray ribbon) complex with CMID-wt (green ribbon) and the model structure obtained by docking simulation of CMID-dSt (**4**, orange ribbon). FA changes of TMR-CMID peptides (100 nM) after the addition of His-MYC3-FLAG (0–2 μM) (c) or His-EIN3-FLAG (0–2 μM) (d). Experiments were performed in triplicate to obtain the mean and SD (shown as error bars) (**1**: open circle, **2**: open square, **3**: cross, and **4**: filled circle). e) Inhibition curves of TMR-CMID peptides (0–3 μM) for biotin-MED25^{CMIDM} (150 nM) and His-MYC3-FLAG (50 nM, open circle) or His-EIN3-FLAG (50 nM, cross) using AlphaLISA assay. Experiments were performed in triplicate to obtain the mean and SD (shown as error bars).

sequences of MYC2 (55–259) or MYC4 (55–253) were highly homologous to MYC3 (44–238) (Fig. S9, sequence homology = 59.7 and 73.9% for MYC2/3 and MYC3/4, respectively), and the 3D structures predicted by AlphaFold2 were also very similar (Fig. S10, RMSD = 1.116 and 1.301 Å for MYC2/3 and MYC3/4, respectively). These results suggest that JAZ10^{CMID} binds to MYC2 or MYC4 in a similar secondary structure, with two helices for desensitization, similar to MYC3. However, notably, the K_d values of **2**, **3**, and **4** with His-EIN3-FLAG changed slightly or even weakened compared to those of JAZ10^{CMID}-wt (290, 600, and 105 nM for **2**, **3**, and **4**, respectively, as shown in Fig. 2d and Table S5). Similar results were also obtained using His-EIL1-FLAG (K_d values of **1** and **4** were 440 and 116 nM, respectively, Table S5, Figs. S11 and S12), suggesting that JAZ10^{CMID} binds to EIN3/EIL1 in a significantly different conformation or interaction site than when MYCs are the binding partners.

Next, we examined the inhibitory effects of JAZ10^{CMID}-based peptides on the disruption of the TFs/MED25 complex, which is required to activate JA signaling in vitro. As previously reported, the PPI between the short binding domain of MED25 (CMID-like MYC-interacting domain [CMIDM]) and MYC3 or EIN3 can be directly observed by the AlphaLISA assay (24, 28); therefore, we used it for the JA-related TF inhibitor assay of our double-stapled peptide **4**. As shown in Fig. 2e, after the addition of **4** to the complex of biotin-conjugated MED25^{CMIDM}/His-MYC3-FLAG, the binding signal decreased in a dose-dependent manner, and the K_i value was 71 nM (Table S5). In contrast, significantly low inhibitory effects of EIN3 were observed (K_i = 1.08 μM) (Fig. 2e and Table S5). All the results demonstrated that we successfully developed a good candidate for MYC family-selective inhibitor based on the 3D structure of JAZ10^{CMID}, at least in vitro.

Inhibitory effects of JAZ10^{CMID}-based stapled peptides in *A. thaliana*

Having identified a MYC family-selective peptide inhibitor in vitro, we assessed the inhibitory effect of stapled peptides **4** on JA responses in *A. thaliana*. Growth inhibition and glucosinolate accumulation are well-known responses induced by JAs via MYC TFs (11, 14). As previously reported, treatment with MeJA caused a severe root growth inhibition in 7-day-old *A. thaliana* seedlings, whereas co-treatment with compound **4** partially suppressed the growth inhibitory effects of MeJA (Fig. 3a and b). Similarly, MeJA-triggered glucosinolate accumulation was significantly suppressed by co-treatment with **4** (Fig. 3c), suggesting that **4** can function as an inhibitor of MYCs, even in plants.

To reveal the mode-of-action of our stapled peptide inhibitor in *Arabidopsis*, we next examined the inhibitory effect of **4** on MeJA-triggered gene expression. As shown in Fig. S13a–d, MeJA-induced expression of MYC-mediated marker genes, such as *VSP2*, *AOS*, *OPR3*, or *MYC2*, was significantly suppressed by co-treatment of **4** with MeJA (11, 43). Conversely, **4** and MeJA strongly activated the expression of *PDF1.2*, an EIN3/EIL1-mediated marker gene (defense responses against necrotrophic pathogens), compared with MeJA treatment alone (Fig. S13e) (25, 44). The expression of other EIN3/EIL1-marker genes, such as *ORA59* and *ACT*, was also activated by co-treatment of **4** with MeJA (Fig. S13f and g). In addition, **4** alone showed almost no effects in the marker gene expression (Fig. S14). This intriguing phenomenon could be explained by a crosstalk regulatory system between MYCs and EIN3/EIL1; MYC-selective inhibition by **4** releases the inherent MYC-mediated repression of EIN3/EIL1 under MeJA treatment (25, 29, 30, 45). To verify this hypothesis, we examined the

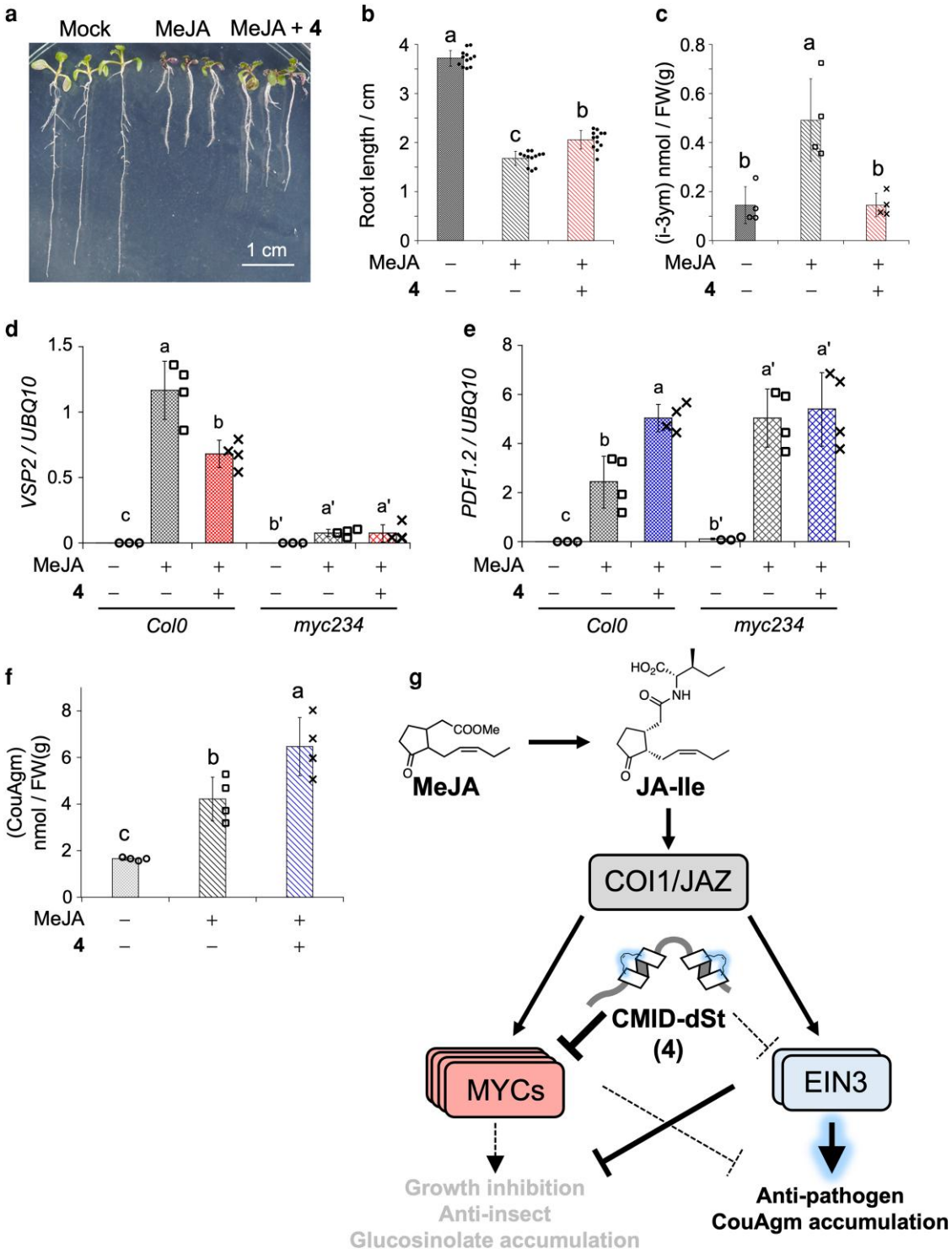

Fig. 3. Inhibitory effects of the designed stapled peptide **4** co-treatment with MeJA in *A. thaliana*. a) *Arabidopsis* seedlings (Col-0) grown for 7 days on a 1/2 MS medium containing MeJA (50 μM) in the presence or absence of **4** (10 μM) treatment for 4 days. Scale bar 1 cm. b) Quantification of root length of the whole seedling in chemicals-treated seedlings shown in (a) ($n = 15$). c) Glucobrassicin (i-3ym) accumulation in 7-day-old *Arabidopsis* seedlings (Col-0) treated with MeJA (50 μM) in the presence or absence of **4** (10 μM) ($n = 4$) treatment for 4 days. d), e) Analysis of JA-responsive gene expression using RT-qPCR in 7-day-old *Arabidopsis* seedlings (Col-0 or *myc234*) treated with MeJA (50 μM) in the presence or absence of **4** (10 μM) ($n = 4$) treatment for 8 h (d: *VSP2*, e: *PDF1.2*). f) *p*-Coumaroyl agmatine (CouAgm) accumulation in 7-day-old *Arabidopsis* seedlings (Col-0) treated with MeJA (50 μM) in the presence or absence of **4** (10 μM) ($n = 4$) treatment for 4 days. All the experiments shown in this figure were repeated three times with similar results, and significant differences were evaluated using a one-way ANOVA/Tukey's HSD post hoc test ($P < 0.01$). g) A predictive diagram showing how a designed stapled peptide **4** selectively suppresses the TFs MYCs but not EIN3/EIL1. **4** can selectively suppress MYC-downstream responses (bold line), and EIN3/EIL1-downstream responses were inherently suppressed by MYCs (dotted line), resulting in **4** activating the EIN3/EIL1-downstream responses.

expression profile of *VSP2* or *PDF1.2* in the MYC triple mutant (*myc234*) (11). As previously reported, the expression of *VSP2* was almost completely abolished after MeJA treatment on *myc234*, whereas that of *PDF1.2* was notably enhanced after MeJA treatment on *myc234* compared to wild-type plants (Fig. 3d and e). Moreover, co-treatment **4** with MeJA did not significantly change the expression pattern of either marker gene on *myc234* compared to MeJA alone. Also, co-treatment of **4** with MeJA on *ein2-1* mutant, an up-stream TF of EIN3/EIL1, did not significantly change the expression pattern of these marker genes (*VSP2* and *PDF1.2*) compared to MeJA alone (Fig. S15). These results indicated that there were almost no off-target effects of **4** other than MYC.

One of the EIN3/EIL1-mediated marker genes, *ACT*, encodes a key enzyme for the biosynthesis of *p*-coumaroyl agmatine, a secondary metabolite involved in the defense of plants against pathogens (46, 47). Therefore, we examined the effect of **4** on the MeJA-triggered accumulation of *p*-coumaroyl agmatine. As shown in Fig. 3f, it was significantly enhanced by co-treatment **4** with MeJA compared to MeJA alone, indicating that the uncoupling effect of **4** toward the crosstalk between MYCs and EIN3/EIL1 was sufficiently strong and phenotypically manifested. All the results obtained in the examinations with *A. thaliana* demonstrated that **4** is an effective inhibitor of the MYC family but not of EIN3/EIL1. Additionally, the MYC family-selective inhibitor **4** uncoupled the crosstalk between MYCs and EIN3/EIL1 (Fig. 3g).

AtJAZ10^{CMID}-based stapled peptide works as a selective chemical inhibitor for MYCs in different plants (*M. polymorpha*)

Analysis of the liverwort *M. polymorpha* genome and functional analyses of the COI1/JAZ co-receptor and MYC TF showed that the JA signaling pathway first appeared more than 450 million years ago (48–51). Nevertheless, bryophytes including liverwort neither synthesize nor respond to JA-Ile, and recently, two isomeric forms of the JA-Ile precursor dinor-*cis*-12-oxo phytodienoic acid (OPDA) (dn-cis-OPDA and dn-iso-OPDA) have been identified in *M. polymorpha* as bioactive ligands of MpCOI1 (48, 52). The functional conservation of the co-receptor COI1/JAZ in bryophytes suggests that, evolutionarily, the JA pathway may have appeared during plant terrestrialization. In contrast, two MYC genes *MpMYC-X* and *MpMYC-Y* are encoded by the *M. polymorpha* sex chromosomes and have revealed that they are orthologs to Arabidopsis MYC TFs, with a similar function in regulating the activation of the JA pathway in *M. polymorpha* (49). As shown in this example, *MYC* is highly conserved in various plant species, such as rice, tomato, and tobacco, although it tends to become more genetically redundant during evolution (53). Specifically, our peptide-based inhibitor, which showed inhibitory effects against all redundant MYC2, 3, and 4 in *A. thaliana*, is expected to apply to various plant species.

To test this hypothesis, we compared the sequences and 3D structure of MYC3 of *A. thaliana* MYC3 (AtMYC3) and *M. polymorpha* (MpMYC-Y). As shown in Fig. S16, the primary sequences of AtMYC3(44–238) and MpMYC-Y were moderately conserved, with 40% homology. In contrast, the predicted structure of MpMYC-Y by AlphaFold2 was very similar to AtMYC3(44–238) (Fig. S17, the RMSD value is 2.181 Å between AtMYC3(44–238) and MpMYC-Y(102–299)). Although a previous bioinformatics study suggested that the CMID domain of AtJAZ10 appeared in angiosperms for the first time, and it is only weakly conserved in higher plants (54), we performed an in silico molecular docking simulation for the predicted structure of MpMYC-Y with **4**. One of the predicted structures of the complex showed that the stapled peptide **4** could bind to MpMYC-Y, similar to the case of **4** with AtMYC3 (Fig. 4a). These results suggest that our stapled peptide can potentially be a MYC-selective inhibitor in *M. polymorpha* and *A. thaliana*.

Next, we examined the binding affinity of the non-stapled peptide AtJAZ10^{CMID}-wt **1** and stapled peptide **4** with MpMYC-Y. The K_d value of **1** with MpMYC-Y was 830 nM (Figs. 4b and S18), which is comparable to that with AtMYC3 (350 nM), whereas the K_d value of **4** with MpMYC-Y was 18 nM (Fig. 4b), which was 46-fold lower than **1** with MpMYC-Y. In contrast, the K_d value of **4** with MpEIN3, an ortholog of AtEIN3 in *M. polymorpha* (Fig. S19) (55), was not significantly different from that of **1** (370 nM for **1** and 89 nM for **4**; Fig. S20).

We examined the inhibitory effect of **4** on OPDA-triggered growth inhibition and gene expression in *M. polymorpha* instead of *A. thaliana*. As previously reported, treatment with OPDA, a precursor of dinor-OPDA, inhibited plant growth, whereas co-treatment with compound **4** partially suppressed the growth inhibitory effects of OPDA (Fig. 4c and d). In addition, as shown in Figs. 4e and S21a, the OPDA-induced expression of MpMYC-mediated marker genes, such as *MpPATATIN*, *MpDIRIGENT LIKE PROTEIN*, and *MpbHLH62*, was significantly suppressed by co-treatment with OPDA and **4** (49). In contrast, **4** with OPDA activated the expression of *MpERF21* and *MpERF1*, which are MpEIN3-mediated marker genes, compared with OPDA treatment alone (Figs. 4f and S21b). Using the MpMYC-Y knockout mutant *mpmycy*, the bioactivity of **4** was completely abolished, indicating that **4** had almost no off-target effects other than those of MpMYC (Fig. 4e and f) (49). These results demonstrate that peptide **4** functions as a selective inhibitor of MYC in *M. polymorpha*.

Discussion

IDP/IDR can adopt various 3D structures in solution and change shape depending on the binding partner. This property allows it to be a key regulator in many intracellular processes involving PPIs, such as signal transduction or liquid–liquid phase separation; therefore, IDP/IDR is currently attracting much attention as an essential drug target (38). IDP/IDR plays a crucial role as a key component of the JA and ET signaling pathways. The C-terminal region of the transcription repressor JAZ in JA signaling, the Jas motif, is an IDR, and it binds to various TFs (MYC family, EIN3, and so on) as well as to the JA receptor COI1 (15). As we previously reported, the JAZ9^{Jas}-derived double-stapled peptide (JAZ9^{Jas}-dSt) selectively binds and inhibits the MYC family, but not COI1, with its ligand JA-Ile (36). However, this was additionally confirmed herein that there is no difference in the affinity of JAZ9^{Jas}-dSt between MYC3 and EIN3 (Fig. S22 and Table S6), indicating that both TFs bind to the Jas motif in a similar helical structure. This study confirmed that JAZ10^{CMID} is also an IDR and binds to both MYC2/3/4 and EIN3/EIL1, whereas the JAZ10^{CMID}-derived stapled peptide (JAZ10^{CMID}-dSt, **4**) selectively inhibits MYC2/3/4 but not EIN3/EIL1 in vivo or in vitro. Since both the AlphaFold and secondary structure prediction methods have shown that EIN3 would contain many parts predicted to be IDRs in its sequence (Fig. S23), it remains unclear how these Jas motif and CMID of JAZ protein would bind to EIN3 at the present. However, our results indicated that chemical fixation of the disordered conformation of IDRs can restrict their original multiple targets, as IDRs change their 3D structure or site depending on their binding partners (Fig. S24) (56). This concept of "chemically redesigned IDR peptide" could provide versatile and beneficial tools effective for modulation of PPI networks in the near future.

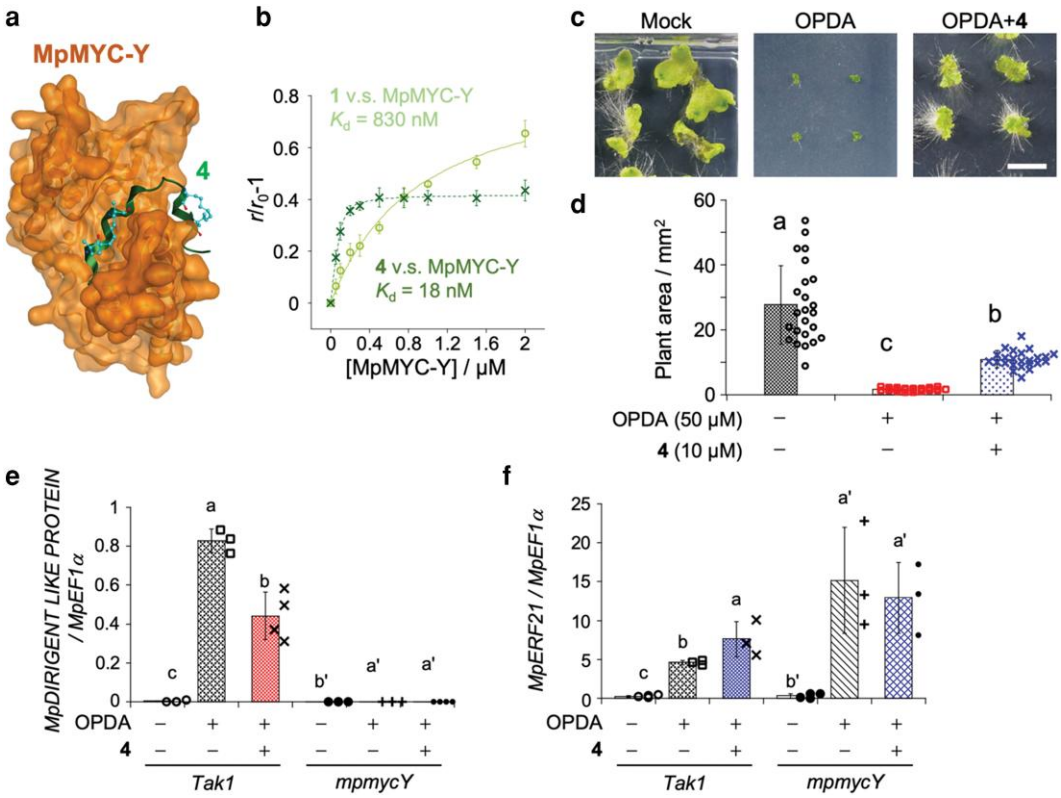

Fig. 4. In vitro and in vivo inhibitory effects of the designed stapled peptide **4** in *M. polymorpha*. a) The model structure obtained by docking simulation of CMID-dSt (**4**, green ribbon) complexed with the predicted structure of MpMYC-Y using AlphaFold2. b) FA changes of TMR-CMID peptides (100 nM, **1** [open circle] or **4** [cross]) after the addition of His-MpMYC-Y-FLAG (0–2 μM). c) *M. polymorpha* gemmalings (Tak-1) grown for 2 weeks on a 1/2 B5 medium containing OPDA (50 μM) in the presence or absence of **4** (10 μM) treatments. Scale bar 0.5 cm. d) Quantification of the plant area (mm^2) of the chemicals-treated seedlings shown in (c) ($n = 24$). e), f) Analysis of JA-responsive gene expression by RT-qPCR in 7-day-old *Marchantia* gemmalings (Tak-1 or *mpmycY*) treated with OPDA (50 μM) in the presence or absence of **4** (10 μM) ($n = 3$ or 4) treatment for 6 h (e: *MpDIRIGENT LIKE PROTEIN*, f: *MpERF21*). All the experiments shown in this figure were repeated three times with similar results, and significant differences were evaluated using a one-way ANOVA/Tukey's HSD post hoc test ($P < 0.01$).

Conclusion

In summary, the designed JAZ10^{CMID}-dSt binds with relatively high affinity to the target TF family AtMYC2/3/4 and MpMYC-X/Y compared to AtEIN3/EIL1 and MpEIN3 (Figs. 2c–e, 4b and Table S5). With such comprehensive selectivity to the target MYC TF family, this peptide effectively suppressed MYC2/3/4-downstream responses and activated EIN3-downstream ones (Fig. 3). This strongly suggests that the crosstalk between the two phytohormone signaling pathways can be modulated by TF-selective chemical tools. Almost all plant hormones interact with each other synergistically or antagonistically through direct or indirect PPI of their respective key TFs, such as MYC2/3/4 in JA signaling, EIN3/EIL1 in ET signaling, PHYTOCHROME INTERACTING FACTOR (PIF) in gibberellic acid (GA) signaling, AUXIN RESPONSE FACTOR (ARF) in auxin signaling, ABSCISIC ACID INSENSITIVE (ABI) in abscisic acid (ABA) signaling, and NONEXPRESSOR OF PR GENES 1 (NPR1) in salicylic acid (SA) signaling (1, 2). Therefore, the design strategy for selective peptide inhibitors for TFs reported in this study should promote peptide inhibitor development research in plant biology.

Phytohormone crosstalk mechanisms have been well characterized in *Arabidopsis* but not in other plants, including various non-model plants. In this study, we successfully demonstrated the existence of a crosstalk mechanism between JA and ET in *Marchantia* using the MYC-selective inhibitor **4**, which has not yet been analyzed (Fig. S21). These crosstalk regulatory systems were also confirmed in the knockout mutant *mpmyc-Y* (Fig. 4e and f), proving that the JA and ET crosstalk regulatory system is conserved in both *Mp* and *At*. Most importantly, demonstrating such crosstalk between plant hormones using chemical tools does not require genetic manipulation. Therefore, it is highly plausible that TF-selective chemical tools will be useful for analyzing crosstalk between plant hormones in non-model plants in the future.

Acknowledgments

The authors thank Prof. G. Howe and Dr J. Yao (Michigan State University, USA) for providing the plasmids of *pEarleygate-35S: JAZ10.4-YFP* for the transformation of *Arabidopsis* and Prof. R. Solano and Dr A. Chini (National Centre for Biotechnology [CNB], Spain) for providing the seeds of *myc234* mutant and gemmalings of *mpmycY* mutant. The authors also thank Dr A. Idei, Dr K. Mino, and Prof. M. Yoshida (RIKEN) for their kind help with the design of the AlphaScreen assays; Ms M. Sasaki, Dr A. Yoda, Dr A. Komatsu, and Prof. J. Kyodzuka (Tohoku University, Japan) for their kind help with *Marchantia* experiments; Dr Y. Sato and Prof. S. Nishizawa (Tohoku University, Japan) for the use of the circular dichroism spectrometer; Mr. S. Xu and Prof. A. Onoda (Hokkaido University, Japan) for their kind help with the prediction of secondary structures of the proteins; and Mr. Q. Li, and Mr. Y. Onodera (Tohoku University, Japan) for their technical assistance. The authors would like to thank Editage (www.editage.jp) for English language editing.

Supplementary Material

Supplementary material is available at *PNAS Nexus* online.

Funding

This work was financially supported by a Grant-in-Aid for Scientific Research from Japan Society for the Promotion of Science (JSPS) (nos. 23K17371, 22H02206, and 21H00270 to Y.T., nos. 23H00316, 23H04883, 22KK0076, 21K19037, 20H00402, JPJSBP120229905, and JPJSBP120239903 to M.U.), Japan Science and Technology (JST) Support for Pioneering Research Initiated by the Next Generation (SPRING) (no. JPMJFS2102 to R.L.), and the Takeda Science Foundation (to Y.T.).

Author Contributions

Y.T. designed research and wrote the paper. Y.T. and R.L. performed research, contributed new reagents, and analyzed the data. Y.T. and M.U. were involved in funding acquisition. All authors reviewed and edited the paper.

Data Availability

All analyzed data needed to evaluate the conclusions in the paper are present in the manuscript and supplementary materials available at *PNAS Nexus* online.

References

1 Riechmann JL, Ratcliffe OJ. 2000. A genomic perspective on plant transcription factors. *Curr Opin Plant Biol*. 3:423–434.
2 Strader L, Weijers D, Wagner D. 2022. Plant transcription factors—being in the right place with the right company. *Curr Opin Plant Biol*. 65:102136.
3 Fujita M, *et al.* 2006. Crosstalk between abiotic and biotic stress responses: a current view from the points of convergence in the stress signaling networks. *Curr Opin Plant Biol*. 9:436–442.
4 Kohli A, Sreenivasulu N, Lakshmanan P, Kumar PP. 2013. The phytohormone crosstalk paradigm takes center stage in understanding how plants respond to abiotic stresses. *Plant Cell Rep*. 32:945–957.
5 Wasternack C, Hause B. 2013. Jasmonates: biosynthesis, perception, signal transduction and action in plant stress response, growth and development. An update to the 2007 review in Annals of Botany. *Ann Bot*. 111:1021–1058.
6 Chini A, *et al.* 2007. The JAZ family of repressors is the missing link in jasmonate signalling. *Nature*. 448:666–671.
7 Thines B, *et al.* 2007. JAZ repressor proteins are targets of the SCFCOI1 complex during jasmonate signalling. *Nature*. 448:661–665.
8 Thireault C, *et al.* 2015. Repression of jasmonate signaling by a non-TIFY JAZ protein in Arabidopsis. *Plant J*. 82:669–679.
9 Gao C, *et al.* 2016. MYC2, MYC3, and MYC4 function redundantly in seed storage protein accumulation in Arabidopsis. *Plant Physiol Biochem*. 108:63–70.
10 Fernandez-Calvo P, *et al.* 2011. The Arabidopsis bHLH transcription factors MYC3 and MYC4 are targets of JAZ repressors and act additively with MYC2 in the activation of jasmonate responses. *Plant Cell*. 23:701–715.
11 Schweizer F, *et al.* 2013. Arabidopsis basic helix-loop-helix transcription factors MYC2, MYC3, and MYC4 regulate glucosinolate biosynthesis, insect performance, and feeding behavior. *Plant Cell*. 25:3117–3132.
12 Huang C-F, *et al.* 2017. Elevated auxin biosynthesis and transport underlie high vein density in C_4 leaves. *Proc Natl Acad Sci U S A*. 114:E6884–E6891.
13 Zhuo M, Sakuraba Y, Yanagisawa S. 2020. A jasmonate-activated MYC2–Dof2.1–MYC2 transcriptional loop promotes leaf senescence in Arabidopsis. *Plant Cell*. 32:242–262.
14 Fonseca S, *et al.* 2009. (+)-7-iso-Jasmonoyl-L-isoleucine is the endogenous bioactive jasmonate. *Nat Chem Biol*. 5:344–350.
15 Sheard LB, *et al.* 2010. Jasmonate perception by inositol-phosphate-potentiated COI1-JAZ co-receptor. *Nature*. 468:400–405.
16 Pauwels L, Goossens A. 2011. The JAZ proteins: a crucial interface in the jasmonate signaling cascade. *Plant Cell*. 23:3089–3100.
17 Chen R, *et al.* 2012. The Arabidopsis mediator subunit MED25 differentially regulates jasmonate and abscisic acid signaling through interacting with the MYC2 and ABI5 transcription factors. *Plant Cell*. 24:2898–2916.
18 Cevik V, *et al.* 2012. MEDIATOR25 acts as an integrative hub for the regulation of jasmonate-responsive gene expression in Arabidopsis. *Plant Physiol*. 160:541–555.
19 An C, *et al.* 2017. Mediator subunit MED25 links the jasmonate receptor to transcriptionally active chromatin. *Proc Natl Acad Sci U S A*. 114:E8930–E8939.
20 Chung HS, Howe GA. 2009. A critical role for the TIFY motif in repression of jasmonate signaling by a stabilized splice variant of the JASMONATE ZIM-domain protein JAZ10 in Arabidopsis. *Plant Cell*. 21:131–145.
21 Chung HS, *et al.* 2010. Alternative splicing expands the repertoire of dominant JAZ repressors of jasmonate signaling. *Plant J*. 63:613–622.
22 Moreno JE, *et al.* 2013. Negative feedback control of jasmonate signaling by an alternative splice variant of JAZ10. *Plant Physiol*. 162:1006–1017.
23 Zhang F, *et al.* 2017. Structural insights into alternative splicing-mediated desensitization of jasmonate signaling. *Proc Natl Acad Sci U S A*. 114:1720–1725.
24 Takaoka Y, *et al.* 2022. Protein-protein interactions between jasmonate-related master regulator MYC and transcriptional mediator MED25 depend on a short binding domain. *J Biol Chem*. 298:101504.
25 Zhu Z, *et al.* 2011. Derepression of ethylene-stabilized transcription factors (EIN3/EIL1) mediates jasmonate and ethylene signaling synergy in Arabidopsis. *Proc Natl Acad Sci U S A*. 108:12539–12544.
26 Zhang X, *et al.* 2018. Integrated regulation of apical hook development by transcriptional coupling of EIN3/EIL1 and PIFs in Arabidopsis. *Plant Cell*. 30:1971–1988.
27 Yang Y, *et al.* 2014. The Arabidopsis mediator subunit MED16 regulates iron homeostasis by associating with EIN3/EIL1 through subunit MED25. *Plant J*. 77:838–851.
28 Liu R, Niimi H, Ueda M, Takaoka Y. 2022. Coordinately regulated transcription factors EIN3/EIL1 and MYCs in ethylene and jasmonate signaling interact with the same domain of MED25. *Biosci Biotechnol Biochem*. 86:1405–1412.
29 Zhang X, *et al.* 2014. Jasmonate-activated MYC2 represses ETHYLENE INSENSITIVE3 activity to antagonize ethylene-promoted apical hook formation in Arabidopsis. *Plant Cell*. 26:1105–1117.
30 Song S, *et al.* 2014. Interaction between MYC2 and ETHYLENE INSENSITIVE3 modulates antagonism between jasmonate and ethylene signaling in Arabidopsis. *Plant Cell*. 26:263–279.

31 Zhang F, *et al.* 2015. Structural basis of JAZ repression of MYC transcription factors in jasmonate signalling. *Nature*. 525: 269–273.
32 Jumper J, *et al.* 2021. Highly accurate protein structure prediction with AlphaFold. *Nature*. 596:583–589.
33 Mirdita M, *et al.* 2022. ColabFold: making protein folding accessible to all. *Nat Methods*. 19:679–682.
34 Hu G, *et al.* 2021. flDPnn: accurate intrinsic disorder prediction with putative propensities of disorder functions. *Nat Commun*. 12:4438.
35 Xu S, Onoda A. 2023. Accurate and fast prediction of intrinsically disordered protein by multiple protein language models and ensemble learning. *J Chem Inf Model*. 64:2901–2911. doi:10.1021/acs.jcim.3c01202
36 Suzuki K, Takaoka Y, Ueda M. 2021. Rational design of a stapled JAZ9 peptide inhibiting protein–protein interaction of a plant transcription factor. *RSC Chem Biol*. 2:499–502.
37 Alderson TR, Pritisanac I, Kolaric D, Moses AM, Forman-Kay JD. 2023. Systematic identification of conditionally folded intrinsically disordered regions by AlphaFold2. *Proc Natl Acad Sci U S A*. 120:e2304302120.
38 van der Lee R, *et al.* 2014. Classification of intrinsically disordered regions and proteins. *Chem Rev*. 114:6589–6631.
39 Sugase K, Dyson HJ, Wright PE. 2007. Mechanism of coupled folding and binding of an intrinsically disordered protein. *Nature*. 447:1021–1025.
40 Schafmeister CE, Po J, Verdine GL. 2000. An all-hydrocarbon cross-linking system for enhancing the helicity and metabolic stability of peptides. *J Am Chem Soc*. 122:5891–5892.
41 Kim YW, Grossmann TN, Verdine GL. 2011. Synthesis of all-hydrocarbon stapled alpha-helical peptides by ring-closing olefin metathesis. *Nat Protoc*. 6:761–771.
42 Kim Y-W, Kutchukian PS, Verdine GL. 2010. Introduction of all-hydrocarbon i, i+3 stapleds into α-helices via ring-closing olefin metathesis. *Org Lett*. 12:3046–3049.
43 Lorenzo O, Chico JM, Sanchez-Serrano JJ, Solano R. 2004. JASMONATE-INSENSITIVE1 encodes a MYC transcription factor essential to discriminate between different jasmonate-regulated defense responses in Arabidopsis. *Plant Cell*. 16:1938–1950.
44 Lorenzo O, Piqueras R, Sanchez-Serrano JJ, Solano R. 2003. ETHYLENE RESPONSE FACTOR1 integrates signals from ethylene and jasmonate pathways in plant defense. *Plant Cell*. 15:165–178.
45 Takaoka Y, *et al.* 2018. A rationally designed JAZ subtype-selective agonist of jasmonate perception. *Nat Commun*. 9:3654.
46 Li J, *et al.* 2018. Jasmonic acid/ethylene signaling coordinates hydroxycinnamic acid amides biosynthesis through ORA59 transcription factor. *Plant J*. 95:444–457.
47 Huang LJ, *et al.* 2022. The AP2/ERF transcription factor ORA59 regulates ethylene-induced phytoalexin synthesis through modulation of an acyltransferase gene expression. *J Cell Physiol*. doi:10.1002/jcp.30935.
48 Kneeshaw S, *et al.* 2022. Ligand diversity contributes to the full activation of the jasmonate pathway in *Marchantia polymorpha*. *Proc Natl Acad Sci U S A*. 119:e2202930119.
49 Penuelas M, *et al.* 2019. Jasmonate-related MYC transcription factors are functionally conserved in *Marchantia polymorpha*. *Plant Cell*. 31:2491–2509.
50 Monte I, *et al.* 2019. A single JAZ repressor controls the jasmonate pathway in *Marchantia polymorpha*. *Mol Plant*. 12:185–198.
51 Monte I, *et al.* 2020. An ancient COI1-independent function for reactive electrophilic oxylipins in thermotolerance. *Curr Biol*. 30: 962–971.e963.
52 Monte I, *et al.* 2018. Ligand-receptor co-evolution shaped the jasmonate pathway in land plants. *Nat Chem Biol*. 14:480–488.
53 Luo L, *et al.* 2023. MYC2: a master switch for plant physiological processes and specialized metabolite synthesis. *Int J Mol Sci*. 24:3511.
54 Garrido-Bigotes A, Valenzuela-Riffo F, Figueroa CR. 2019. Evolutionary analysis of JAZ proteins in plants: an approach in search of the ancestral sequence. *Int J Mol Sci*. 20:5060.
55 Li D, *et al.* 2020. Ethylene-independent functions of the ethylene precursor ACC in *Marchantia polymorpha*. *Nat Plants*. 6:1335–1344.
56 Borcherds W, *et al.* 2014. Disorder and residual helicity alter p53-Mdm2 binding affinity and signaling in cells. *Nat Chem Biol*. 10:1000–1002.